A Community-Oriented Flood Map Visualization and Evaluation Framework

Moiyyad Sufi[1*], Carlos Erazo Ramirez[1,2], Bong-Chul Seo[3], Felipe Quintero[4], Pitamber Wagle [5], Daniel P. Ames[5], E. James Nelson[5], Ibrahim Demir[1,2]

[1] ByWater Institute, Tulane University, New Orleans, LA
[2] River-Coastal Science and Engineering, Tulane University, New Orleans, LA
[3] Civil, Architectural and Environmental Engineering, Missouri University of Science and Technology, Rolla, MO
[4] IIHR-Hydroscience and Engineering, University of Iowa, Iowa City, IA
[5] Civil and Construction Engineering, Brigham Young University, Provo, UT
[*] Corresponding Author, msufi@tulane.edu

Abstract

Flood inundation maps are essential for preparedness, response, and long-term risk mitigation, yet many existing visualization platforms remain limited by rigid data structures and region-specific workflows. This study introduces FIMApp, a client-side, web-based framework and platform for integrating, visualizing, and comprehensively evaluating flood map products using standardized, portable data formats. The system incorporates three data specifications, the FIM Database, FIM Scenario, and FIM Damage formats, which enable interoperable representation of flood extents, near-real-time inundation stages, and property-level impacts. FIMApp supports raster and vector datasets, interactive scenario exploration, model comparison, and browser-based persistence without server dependencies. A comprehensives case study demonstrates the framework's ability to render stage-wise inundation, quantify agreement between HAND and SRH-2D models, and integrate hosted flood datasets (e.g., HydroShare). The results highlight the framework's extensibility, reproducibility, and suitability for flood risk communication. The result is a scalable, community-oriented platform for integrating and analyzing diverse flood mapping products.

Keywords

Flood Inundation Mapping; Web Applications; Hydroinformatics; HydroShare

This manuscript is an EarthArXiv preprint and has been submitted for possible publication in a peer reviewed journal. Please note that this has not been peer-reviewed before and is currently undergoing peer review for the first time. Subsequent versions of this manuscript may have slightly different content.

1. Introduction

Flood events are among the most damaging natural hazards worldwide, with severe consequences for human safety, infrastructure, and economic systems. The frequency and intensity of flood events are increasing as shifting weather patterns produce more extreme precipitation events (Trenberth et al., 2015; Seneviratne et al., 2021). At the same time, continued urban expansion reduces natural infiltration and increases overland flow, further amplifying flood risk. These compounding drivers create evolving conditions that increase the likelihood of widespread flooding and related damage to infrastructure and livelihoods. Effective preparation is therefore essential to mitigate flood impacts, and one of the most valuable preparedness tools is flood inundation map (FIM) visualization systems to understand existing and future flood risk. Such applications provide decision-makers, emergency managers, and the public with actionable information to anticipate hazards, coordinate response efforts, and minimize losses before and during flood events. Beyond emergency situations, flood visualization tools can also support long-term planning decisions related to infrastructure development, land management, insurance policies, and economic risk assessments (Ewing et al., 2022; Erazo Ramirez et al., 2022, 2023; Duran et al., 2025).

Flood impacts depend on both the physical characteristics of a landscape and the hydrologic processes driving an event. In particular, riverine flooding depends on flow contributions from multiple tributaries across a watershed, as well as interactions between upstream and downstream boundary conditions. These dynamics can be analyzed through flood inundation maps generated from hydrologic and hydraulic simulations under different forcing scenarios, including variable precipitation patterns, tributary inflows, and landscape conditions (Li et al., 2025). Traditional FIM products typically focus on a limited set of maps associated with discrete annual exceedance probabilities (e.g., 50%, 10%, or 1%) derived from simulations representing probabilistic rainfall or discharge conditions. While these products provide useful approximations of flood risk, they are not designed to capture the full range of dynamic scenarios that may occur during real events (Cikmaz et al., 2025). Scenario-based analysis frequently requires modifying model drivers to evaluate historical or extreme conditions, which may not be feasible depending on the modeling framework used. As a result, flood model outputs must be communicated through flexible visualization tools that represent diverse scenarios clearly and intuitively.

Recent advances in hydrologic forecasting, hydraulic modeling, and geospatial web technologies have enabled the development of operational flood inundation mapping platforms capable of delivering near–real-time flood information (Hales et al., 2022). In the United States, national-scale flood mapping capabilities have been implemented through systems that couple streamflow forecasts from the National Water Model (NWM) (Cosgrove et al., 2024), whose short-range forecast skill for flood timing and magnitude has been evaluated against observed events (Maghami et al., 2026), with terrain-based inundation approaches such as Height Above Nearest Drainage (HAND) to generate rapid estimates of flood extent across large river networks (Johnson et al., 2019; NOAA Office of Water Prediction, 2025). These approaches provide computationally efficient flood guidance at continental scales and support situational awareness for forecasting

agencies and emergency management operations. However, moving research-grade flood mapping and visualization tools into routine operational use remains a persistent challenge (Ames et al., 2026).

At regional and state levels, more detailed flood mapping systems integrate hydrologic forecasts with hydraulic simulations. The Iowa Flood Information System provides one example, combining hydrologic monitoring networks with inundation maps derived from physical simulations across multiple exceedance probabilities and forecast scenarios (Gilles et al., 2012; Demir et al., 2018). Similar initiatives demonstrate how web-based platforms can integrate forecast data, hydraulic models, and geospatial visualization tools to improve flood awareness and decision support (Ashby et al., 2021; Rojas-Lesmes et al., 2025; Erazo Ramirez & Demir, 2025; Sugiyama et al., 2025).

Hydraulic modeling remains a primary method for generating high-resolution inundation maps. Models such as HEC-RAS (USACE HEC, 2016), TELEMAC-2D (OpenTELEMAC, 2000, 2012), SRH-2D (US Bureau of Reclamation, 2016) and LISFLOOD-FP (Shustikova et al., 2019) simulate floodplain hydraulics using numerical solutions of the shallow-water equations, producing detailed estimates of water depth and velocity (Bates et al., 2010; Neal et al., 2018). While these models provide physically based representations of flood processes and are widely used for engineering analysis and regulatory floodplain mapping, their computational demands can limit their use in large-scale or near-real-time forecasting contexts.

Terrain-based approaches provide a complementary alternative for rapid flood mapping. The HAND method derives inundation extents from digital elevation models by calculating terrain elevation relative to the nearest drainage channel and coupling these values with stage–discharge relationships (Nobre et al., 2011). When integrated with hydrologic forecasts, HAND-based frameworks efficiently generate inundation maps across extensive river networks. Evaluations of this approach indicate that HAND provides reasonable estimates of flood extent in larger river systems but tend to underestimate inundation in smaller channels or complex floodplains (Johnson et al., 2019; Aristizabal et al., 2023).

Alongside modeling developments, web-based visualization systems are a key component of modern flood mapping workflows. Interactive applications enable users to explore flood scenarios, integrate contextual datasets, and communicate flood risk information through browser-based environments (Swain et al., 2016; Ames, 2026; Mahjarin et al., 2026). Previous studies have demonstrated the feasibility of performing flood inundation mapping and visualization directly within client-side web systems using modern geospatial technologies (Li et al., 2022). Additional research has explored methods for incorporating uncertainty and scenario variability in flood mapping platforms, including probabilistic inundation mapping and interactive comparison tools that allow users to evaluate multiple flood scenarios (Li et al., 2023), and disaster risk management through well-established assessment tools ported to the web (Sufi et al., 2025). Data sharing is a significant step toward democratizing these information systems, allowing interested users to leverage tools and datasets created for specific locations (Horsburgh et al., 2015).

Despite these advances, many flood mapping platforms remain tightly coupled to specific datasets, modeling workflows, or geographic regions, limiting their adaptability and reuse. In addition, inundation datasets are often distributed in model-specific formats that do not explicitly encode scenario metadata such as hydrologic forcing, boundary conditions, vertical datum references, or model configuration parameters. This lack of a portable data structure complicates interoperability between modeling systems and visualization tools and restricts the integration of diverse datasets (Oldham et al., 2024; Wagle et al., 2026).

To address these limitations, this study introduces a set of flexible, JSON-based data specifications, designed to encode flood inundation scenario metadata and facilitate consistent representation of inundation datasets. Building on this data structure, we developed a web-based framework that can render, analyze, and evaluate flood inundation scenarios from multiple sources. The rest of the manuscript reads as follows: Section 2 describes the methodology for software architecture and data specification formats; Section 3 presents the case studies and corresponding results and discusses limitations related to browser-based computation, storage, and data accessibility; and Section 4 concludes with final remarks and directions for future work.

2. Methodology

We introduce the Flood Inundation Mapping Application (FIMApp), a web-based, client-side application with a wide range of tools for uploading, visualizing, and analyzing flood maps. FIMApp supports several geospatial file formats and introduces a novel data representation that improves accessibility for flood mapping. The app provides scalable and replicable visualizations of flood inundation maps. Users can generate different flood-extent visualizations from scenarios that combine stage or discharge values at river locations in the domain. The application also enables the visualization of property-level damage estimates for each scenario. In addition to visualization, the application provides utilities to upload, store, and visualize flood inundation or other geospatial files from online databases or local file systems, and to compare inundation maps by analyzing extent against ground truth and simulated scenarios. The software architecture of FIMApp is shown in Figure 1.

FIMApp is organized into two primary components: the File Uploader, and Map Layers. The File Uploader stages and prepares input datasets used for scenario generation, comparative analysis, and visualization. Through the upload interface, users specify the scenario to be rendered. Each module within this component supports multiple file types and serves as the input pipeline for subsequent processing and visualization steps. In addition, the User File functionality enables visualization of user-provided vector or raster datasets that can be uploaded either from an online database or directly from the local file system on the client machine.

The Map Layers component generates spatial visualizations based on uploaded datasets and user-defined parameters. The Flood Extent Scenario, Flood Depth, and Time Series views present map-based layers and associated hydrologic information, including depth-based stage values, volumetric discharge measurements, and flood extent boundaries. The Flood Depth view supports real-time visualization of depth conditions as users modify input parameters. Interactive controls

let users dynamically adjust map extents based on stage–discharge relationships or values derived from time-series data, so the displayed flood conditions update accordingly. The application also includes a scenario comparison function that allows users to evaluate two flood maps generated for the same geographic location. This functionality supports comparing flood extents produced using different generation techniques and/or flood stage values, and it computes spatial overlap metrics to quantify similarities and differences between scenarios.

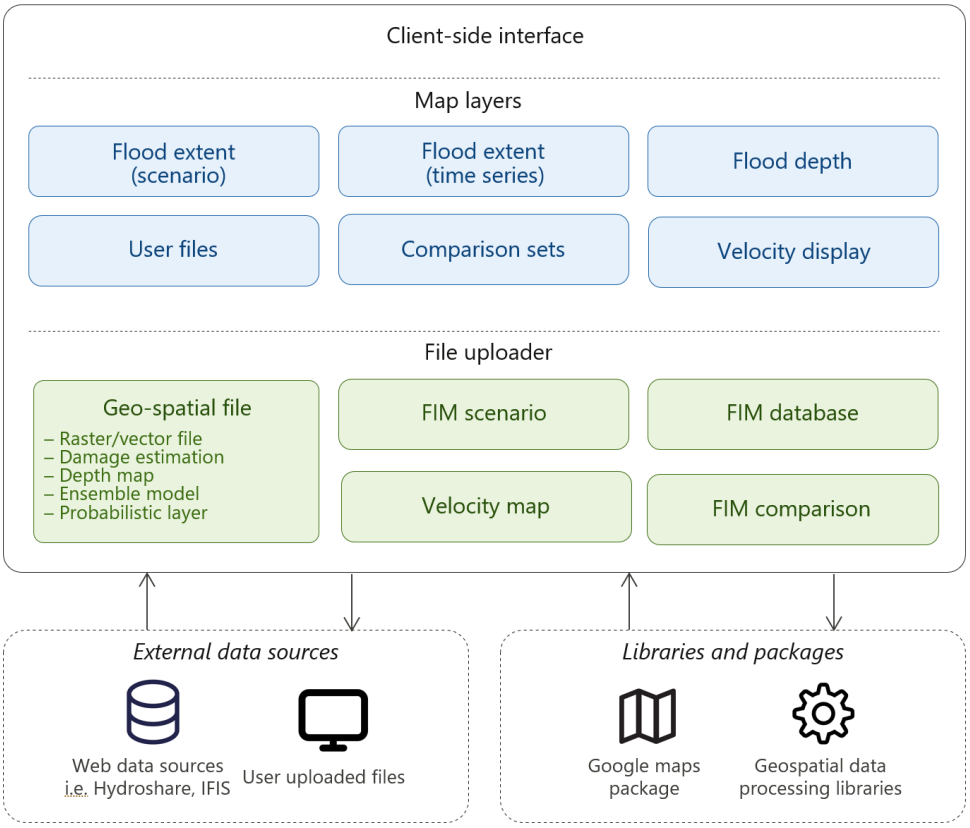


Figure 1. Software architecture of FIMApp. It comprises two core components: Map Layers and File Uploader, each with distinct functions for dynamic dataset ingestion and use.

2.1. Data Specification

The application introduces several portable and reusable data specification formats for storing and transferring flood-related datasets. The first format is the FIM Database Format, which functions as an online catalog for storing and transmitting files efficiently across the web. This format can be integrated into the application via a simple URL, allowing users to access, visualize, and compare flood extent datasets directly. The second format is the FIM Scenario Format, designed to store flood extent information for specific river systems. This format supports both time-series and scenario-based flood analyses and can also include model metadata associated with scenario generation. The third format, the FIM Damage Format, represents estimated property damage associated with a particular flood extent scenario. This file corresponds to a specific flood map

and contains geospatial coordinates along with data describing structural and content damage values, enabling spatial visualization and analysis within the application.

2.1.1. FIM Database Format

The FIM Database format is a lightweight catalog structure used to store references to flood inundation maps and other geospatial datasets that FIMApp can access. Rather than storing the datasets directly within the application, the database maintains a structured list of file references that enable efficient storage, transfer, and retrieval of flood mapping resources over the web. The database is represented as a JSON object (ECMA, 2017), which can either be uploaded directly into FIMApp or retrieved dynamically from a remote server using a provided URL. JSON was selected due to its widespread support in web applications and its flexibility for integrating, modifying, and extending data structures.

Within the database, each dataset is represented as an object contained in a list. These objects use key–value pairs to describe the files available for retrieval. At minimum, each entry contains the following attributes: (i) *FileID* – A unique numeric identifier used to reference the dataset within the catalog; (ii) *FileName* – The name of the geospatial data file, including the file extension. Supported formats include vector datasets (e.g. .shp, .kml, .kmz, .geojson) and raster datasets (e.g., .tif, .geotiff) representing flood extents, flood depths, or water surface elevations. This structure is visualized in Figure 2.

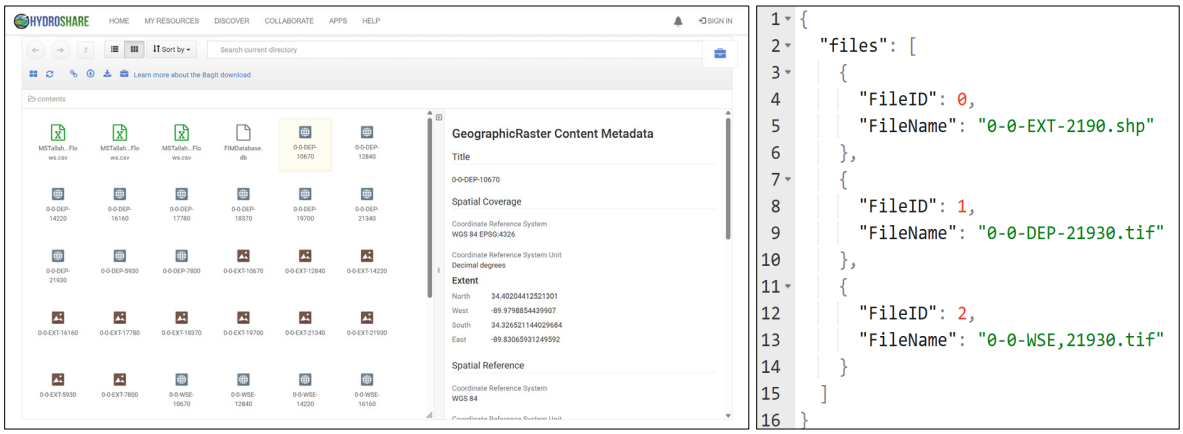


Figure 2. (*Left*) Screenshot of the HydroShare platform showing the BYU FIM Database with a list of available files. (*Right*) An excerpt from the FIMDatabase.json file describing the data structure for the FIM Database format. This self-describing structure lets users provide a simple yet scalable file structure that can be shared across multiple instances.

An example implementation of this structure is provided by the BYU FIM Database (Oldham et al., 2024; Wagle et al., 2026), which is hosted on HydroShare, a web-based platform for sharing hydrologic datasets, models, and related scientific resources (Horsburgh et al., 2015; Tarboton et al., 2024). To retrieve a dataset, FIMApp uses the database retrieval function. The application first loads the JSON database file from a remote location. When a specific dataset is requested, the

retrieval function constructs the file URL by replacing the JSON file name in the base path with the FileName value associated with the selected entry. The application then issues an HTTPS fetch request to retrieve the referenced geospatial file (e.g., a flood extent GeoTIFF). This catalog-based approach allows flood scenario datasets to be stored externally while remaining accessible through a standardized reference structure. As a result, the system supports scalable management of flood mapping resources, promotes reuse of datasets across projects, and simplifies sharing and access to geospatial files for visualization and comparison within web-based flood mapping applications.

2.1.2. FIM Scenario Format

The *Flood Extent Scenario* and *Time Series* components of FIMApp require the ability to manage collections of flood maps for a given location that correspond to either a flood stage series or a time series. In addition to referencing the flood map datasets, the system must store metadata describing each scenario, including the model used to generate associated hydrologic variables such as stage and discharge. To support these requirements, the FIM Scenario format was developed as a simple, replicable, and extensible JSON-based data structure. An overview of this format is presented in Figure 3. The structure primarily consists of a list of scenarios and a list of time-series values. Scenario entries are organized according to the model used to generate the inundation maps, which may include hydrologic, hydraulic, or coupled modeling approaches (Kumar et al., 2023). Within each model group, flood maps are stored under the key scenario_list. Each entry in this list represents an individual flood scenario and contains references to the associated raster or vector flood map files, which can be retrieved and visualized within the application.

```
{
  "location": "<location name>",
  "more_info": "<details and gauge metadata>",
  "scenarios": [
    {
      "model": "<model name>",
      "scenario_list": [
        {
          "vector_file": "<vector file URL>",
          "raster_file": "<raster file URL>",
          "stage": 10,
          "discharge": 10000,
          "annual_exceedence": 25,
          "layer_id": "<ID>"
        }
      ]
    }
  ],
  "time_series": [
    {
      "stage": 8.5,
      "discharge": 9000,
      "timestamp": "2025-01-01 10:00:00",
      "type": "<observed or forecasted value>"
    }
  ]
}
```

Figure 3. Overview of the FIM Scenario file format representing location-wise scenario and time-series information.

In addition to the links to each map, each scenario item contains the following attributes: (i) stage (e.g., 10.0 ft); (ii) discharge (e.g., 10,000 cfs); (iii) annual exceedance (chance) (e.g., 25-year flood event, for instance); and (iv) layer id (unique identifier for each value in the scenario_list). The format includes a time-series array that supports visualization of flood inundation over a specified period. The time series is stored as a list under the time_series key, where each entry represents either observed or forecasted conditions. Each item contains stage, discharge, timestamp, and type (e.g., observed or forecasted) attributes.

Time-series entries do not directly reference a specific flood map or model output. Instead, when a time-series value is selected, the corresponding flood map is determined dynamically by matching the stage value to the closest available scenario stage within the scenario_list of a user-selected model. This approach allows users to visualize historical or forecast stage progression using any modeling method included in the file, enabling time-lapse visualization of flood extents and depths across multiple modeling perspectives.

2.1.3. FIM Damage Format

The FIM Damage Format tracks properties affected during a specific flood scenario and enables visualization of the spatial distribution of community impacts. Each damage file is typically associated with a specific scenario from a user-selected model defined in the flood extent file. This structure supports damage analysis and decision-making by linking property-level impacts directly to modeled flood conditions. This file contains the location, model identifier, and corresponding flood stage data, along with a list of affected properties. The data encoded for each property includes: (i) latitude and longitude coordinates; (ii) content and structural damage percentages (cp, sp) and (iii) content and structural damage dollar amounts (cd, sd). This representation can be used to visualize spatial, depth-damage relationships for property-level damage along with inundation maps and is shown in Figure 4.

```
{
  "location": "<location name>",
  "model": "<model name>",
  "stage": "<associated elevation value>",
  "discharge": "<associated discharge value>",
  "annual_exceedence": "<annual probability of exceedence>",
  "buildings": [
    {
      "id": 1218,
      "lat": 41.964,
      "lng": -91.661,
      "cp": 5,
      "cd": 2029,
      "sp": 6,
      "sd": 4058
    }
  ]
}
```

Figure 4. Sample for the FIM Damage representation. The relevant building information is presented with its location and structural and content damage.

2.2. Map Visualization Layers

FIMApp provides functions to load, manage, and visualize flood inundation scenarios and maps from multiple data sources. The application uses web technologies, including the Google Maps JavaScript API and open-source JavaScript libraries, enabling a portable web-based system that runs in any modern browser on a computer system. Uploaded datasets can be persistently stored using browser-based storage, reducing the need for dedicated server-side storage and lowering system maintenance costs.

The application is designed to be intuitive and extensible using standardized data formats that allow new scenarios and inundation maps to be easily incorporated. Flood maps may be generated using a variety of approaches, including digital elevation modeling techniques such as the HAND model (Thalakkottukara et al., 2024) or hydrodynamic modeling frameworks. These datasets can then be uploaded to FIMApp for visualization and analysis. The system supports a wide range of geospatial data interchange formats, as summarized in Table 1.

Table 1. Description of various geospatial file formats supported to load, visualize, compare and analyze geospatial information in FIMApp.

Data Format	**File Extension**	**Description**
Tagged Image File	.tif or .tiff	TIFF is a raster image format which can contain metadata for exchanging geospatial information. FIMApp currently only supports TIFF files which have a single-band and reprojects uploaded GeoTIFFs to WGS84 automatically, supporting NAD83, the UTM zone families, Web Mercator, NAD83/Conus Albers, and USA Contiguous Albers Equal Area formats
Geographic Tagged Image File	.geotiff	TIFF file format variant which contains specific metadata tags encoding projection information. Like .tif files, FIMApp currently only supports images which are single-banded and reprojects images to WGS84 standard.
Shapefile	.shp	SHP is a vector data format which contains projected coordinate data for one or more geometrical shapes of a single type. Examples of possible shapes are multipoint, polyline and polygon.
Keyhole Markup Language	.kml/.kmz	KML is an XML-encoded vector data format that stores data in 3D geographic coordinates stored in the WGS84 standard. KML files are often distributed in a zipped format with a KMZ file extension.
GeoJSON	.geojson	An open vector data format, GeoJSON represents multiple geographical geometries including points, lines and polygons, and multi-part variants of these types. GeoJSON uses the WGS84 standard to store coordinate data.

2.2.1. Flood Extent (Scenario) Viewer

The Flood Extent (Scenario) functionality allows users to load and interact with scenario-based flood maps associated with a specific community and river body. These maps are pre-encoded using the previously described formats and typically include loading vectors or rasterized data to represent the flood extent pertaining to specified evaluation metrics. Upon selecting a scenario, the application dynamically renders the inundation footprint and displays scenario metadata including: (i) River and Gauge ID; (ii) Flood Level (e.g., stage threshold at which flooding begins); (iii) Date of map generation; (iv) Hydrologic/Hydraulic models used for generating flood map (e.g., HEC-RAS); and (v) Stage and discharge values for the selected scenario. FIMApp has examples of flood extent scenarios for the cities of Cedar Rapids and Des Moines in Iowa available by default, the former of which we have visualized in Figure 5. Further scenarios can be added by uploading data in the FIM Scenario format.

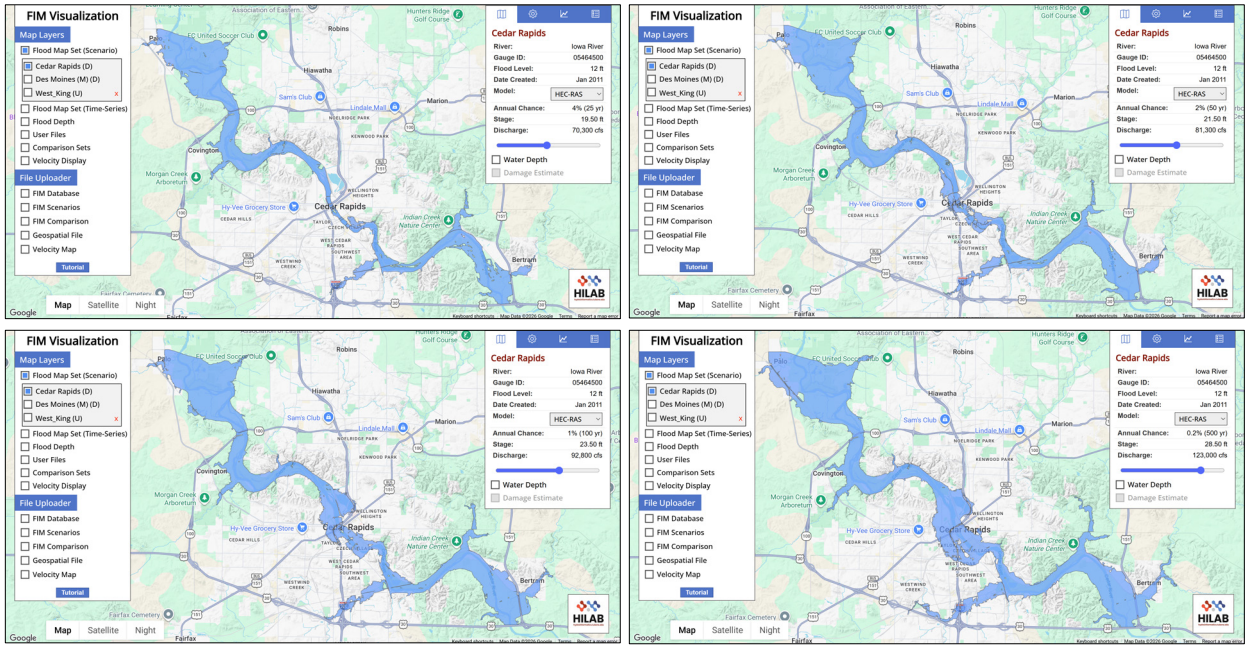


Figure 5. Visualizing 4% (25-year), 2% (50-year), 1% (100-year), and 0.2% (500-year) annual exceedance probability scenarios for Cedar Rapids generated using the HEC-RAS model.

Users can navigate through the range of flood stage values defined within the scenario file, allowing interactive adjustment of the flood extent displayed on the map for comparative analysis. Users may also switch between available modeling approaches, enabling comparison of results produced by different models for the same region one at a time or side by side in two browser windows. When a stage value is selected, the system retrieves the corresponding raster and/or vector dataset via an HTTP fetch request and processes it using an array buffer to support multiple geospatial formats, including Shapefiles, KML, KMZ, and raster datasets. The retrieved data is then rendered within the Google Maps interface using methods provided by the Google Maps API.

The API supports direct loading of GeoJSON and KML/KMZ files through the loadGeoJson method and the KML layer interface, respectively. Raster datasets are rendered through a custom overlay layer implemented by extending the OverlayView class. Because Shapefiles are not directly supported by Google Maps API, they are first converted into a compatible vector format (e.g., GeoJSON) using the SHP.js library prior to visualization.

2.2.2. Flood Extent (Time-Series) Viewer

The Flood Extent (Time Series) function visualizes river stage values over a specified time period for flood maps associated with a particular community. Time-series information is stored within the FIM Scenario data format, enabling dynamic rendering of inundation footprints as stage conditions evolve over time. Each time-series entry contains the following attributes: (i) River and gauge identifier; (ii) Flood level (e.g., stage threshold for flooding); (iii) Date of map generation; (iv) Stage and discharge values; and (v) Timestamp corresponding to the observed or forecasted stage value. FIMApp includes example time-series scenarios for the cities of Cedar Rapids and Des Moines, Iowa, in its default configuration; we have visualized the latter in Figure 6. Additional scenarios can be incorporated by uploading datasets formatted using the FIM Scenario specification.

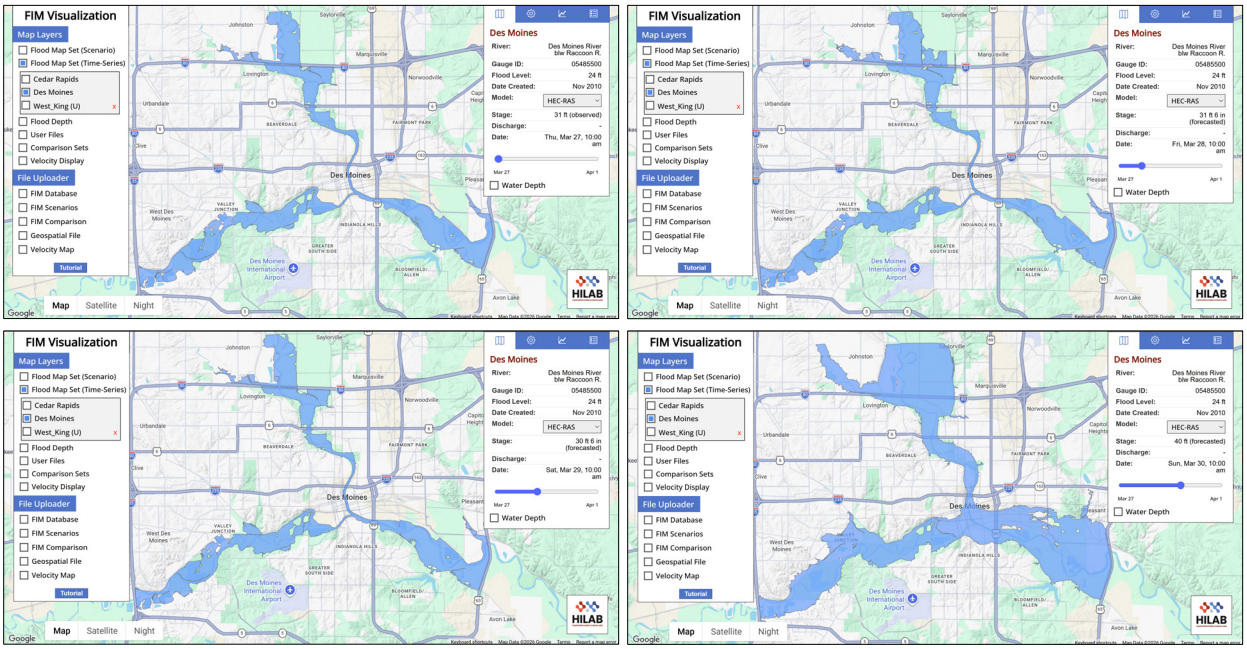


Figure 6. Visualizing time series over a period of 4 days (from March 27th to 30th 2024, increasing left-to-right, then top-to-bottom) for Des Moines River to show river stage evolution for observed and forecasted data. These flood maps are for demonstration purposes, and real river stage values may differ for this time period.

The flood map displayed is determined by matching the selected time-series stage value to the closest available stage value in the scenario list and rendering the corresponding raster or vector

inundation map. Stage values within the time series may represent either observed measurements from sensors or forecasted values generated by hydrologic or hydraulic models. This functionality also allows users to switch between available flood map generation models, enabling comparison of time-series inundation patterns across different modeling approaches. The process for retrieving and rendering inundation maps in Google Maps follows the same mechanism used in the Flood Extent Scenario.

2.2.3. Flood Depth

The Flood Depth layer draws on a flood depth service published by the Iowa Department of Natural Resources (DNR) as an ArcGIS MapServer, which provides flood depth information for specific flood scenarios (Map service, 2025; GIS Analysis & Support, 2025). When the flood depth layer is activated, FIMApp sends a request to the Iowa DNR ArcGIS MapServer using the current geographic bounds of the map view. The server responds with tiled raster data representing inundation depth for the requested region. The system then renders these raster tiles as an overlay on the Google Maps interface, allowing users to visualize spatial variations in flood depth within the selected map extent. An example visualization for a 500-year flood scenario is shown in Figure 7.

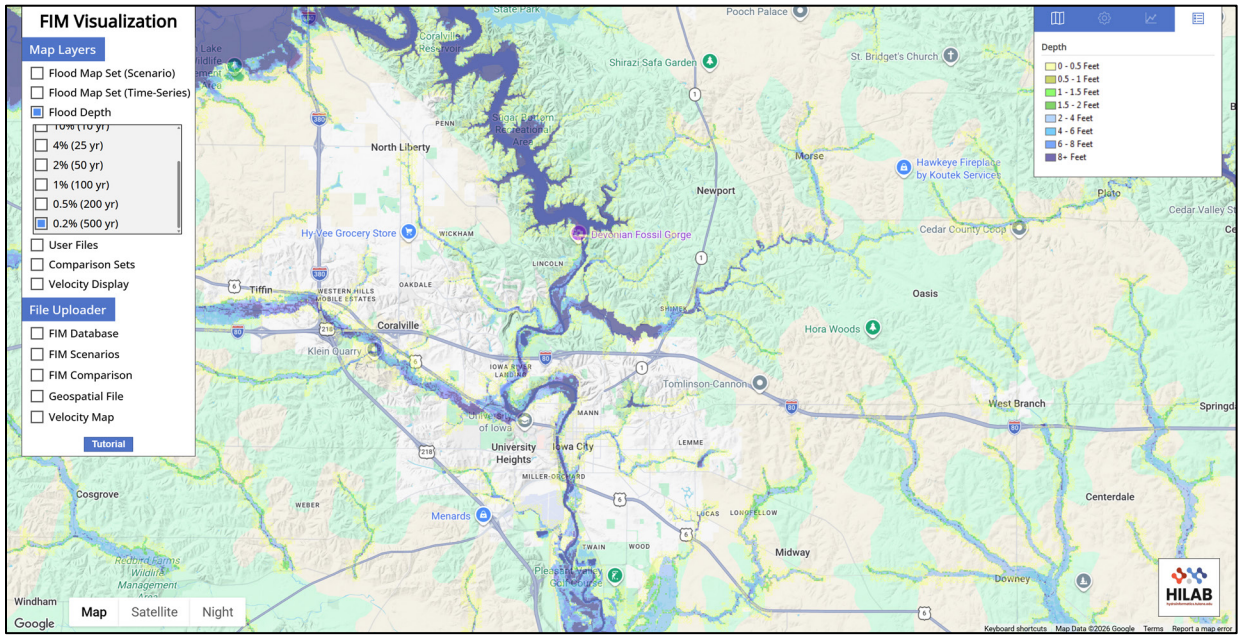


Figure 7. Depth map showing the flood inundation depth for a 0.2% (500 year) flood scenario over Iowa City and Coralville, obtained from ArcGIS Map Server by the Iowa Department of Natural Resources.

2.2.4. Geospatial File Viewer

The Geospatial File Viewer is the general-purpose entry point for loading user-supplied datasets into FIMApp. Users can use this interface to upload different types of files, including vector layers,

raster images, flood-depth grids, ensemble model outputs, and property-level damage datasets. These files can be subsequently managed from the User Files panel. Once accepted, the browser parses each dataset, reprojects it to WGS84 where needed, and stores it in browser-based storage (IndexedDB), so uploaded layers remain available across sessions without server-side storage.

Different file types uploaded to a geospatial file viewer can have different classifications. For vector inputs (JSON, GeoJSON, KML/KMZ and SHP), the user selects between Vector and Damage Layer; for raster inputs (TIFF, GeoTIFF), the user selects between Raster Image, Depth Map, and Ensemble Model. The chosen type is stored alongside the file and determines how the layer is rendered when it is later activated from the User Files panel, similar to the scenario files.

A raster image is a single-band GeoTIFF that does not carry a semantic value scale (for example, a binary inundation mask). On display, the raster is reprojected if required and drawn to an HTML canvas that is positioned on the map through a custom overlay extending the Google Maps OverlayView class.

A depth map is a single-band GeoTIFF whose pixel values encode a continuous flood-inundation depth quantity. Depth layers are rendered through a dedicated depth overlay that applies a graduated color scale to the pixel values and produces a matching legend. This complements the server-hosted depth service described in the Flood Depth subsection by allowing users to load their own depth grids. An example of a depth map is given in Figure 8.

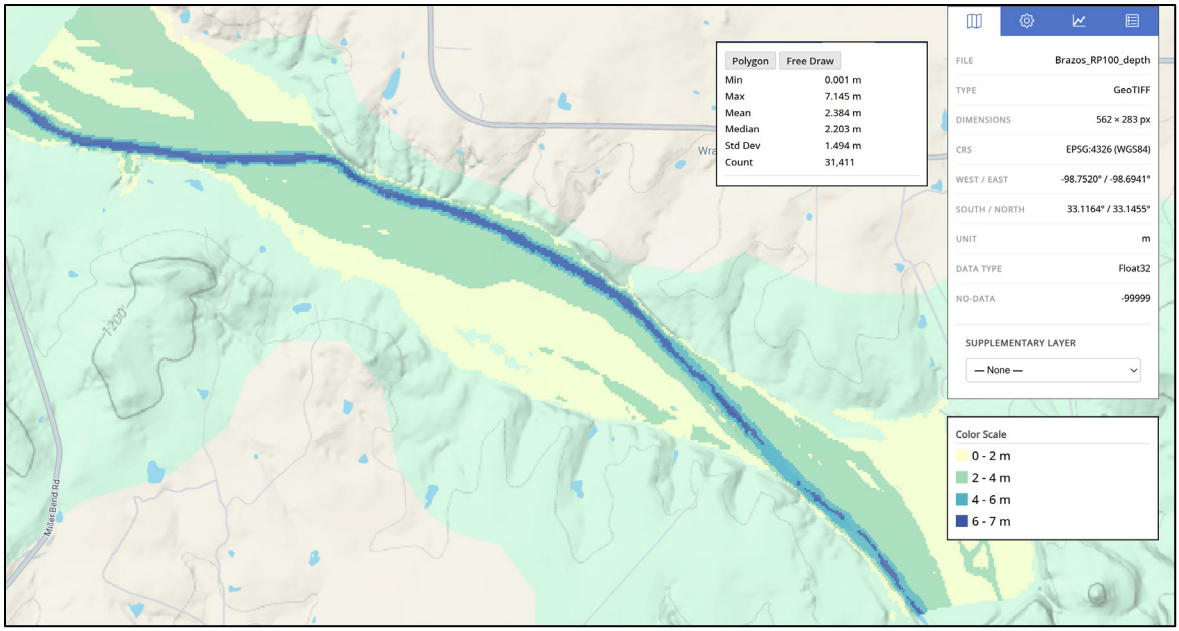


Figure 8. A user-supplied flood-depth GeoTIFF rendered as a Depth Map, with a legend scale derived from the file's embedded metadata.

The final sub-type for TIFF files is ensemble maps. These layers visualize the output of probabilistic or multi-member flood models, in which each pixel carries a class value (for example, an exceedance-probability band or a member-count category) rather than a continuous magnitude.

The GeoTIFF is decoded, and each pixel is colored according to a discrete legend parsed from the file's GDAL_METADATA tag; the legend may be expressed either as discrete values or as value ranges. Where no embedded legend is present, FIMApp derives a fallback legend automatically from the distinct values found in the raster. The resulting classified raster is drawn through an overlay in the same manner as the other raster products, and its class legend appears in the Layer Panel, as shown in Figure 9.

The damage-layer product visualizes property-level flood-damage estimates for a community. It contains structural and content damage values (as percentages and associated monetary loss estimates) for each affected property. These values are typically derived by applying depth-damage relationships developed by local or regional agencies to the properties within the affected area; depth-damage functions describe expected damage per unit area for specific building types and are commonly derived from historical flood-damage observations (Scawthorn et al., 2006).

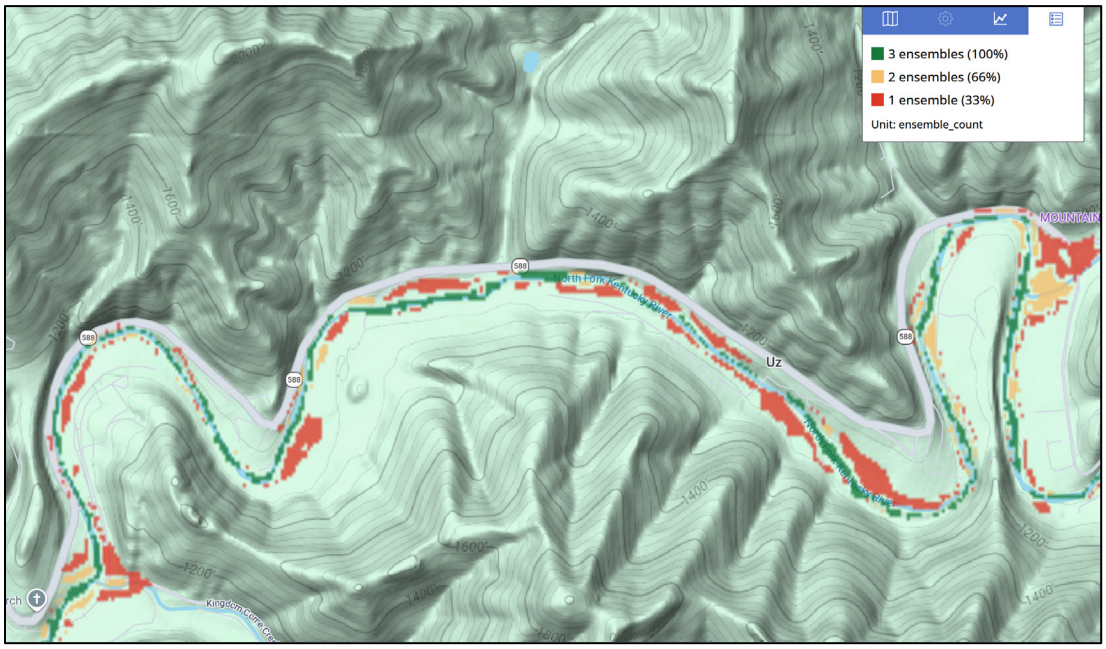


Figure 9. Ensemble agreement map for a section of the North Fork Kentucky River, rendered as a classified raster. Each class represents the number of models predicting inundation at that location, with green for three, orange for two, and red for one model. The class value colors are read from the GDAL_METADATA tag in the file header.

FIMApp accepts damage datasets in two encodings. The first is FIM Damage scenario files in a JSON/GeoJSON file in which each property is represented as a point carrying structural and content damage percentages and dollar values as shown in Figure 10. The second is an OGC GeoPackage (.gpkg) produced by a consequence-analysis workflow. On upload, its point features are converted to GeoJSON in the browser, and per- property attributes like occupancy class, inundation depth, structural and content loss, damage category, and daytime/night-time population by age group are extracted into the same internal representation.

When a damage layer is activated, each property is drawn as a map marker whose color reflects the combined structural and content damage severity, grading from yellow (low) through orange and red to purple (most severe). Clicking a marker opens an information window with the property's detailed breakdown. A summary panel reports the number of affected buildings and the aggregate structural and content damage; for GeoPackage datasets, it additionally reports the total affected population (broken down by daytime/night-time and by the under-/over-65 age groups) and a per-category table of building counts and losses.

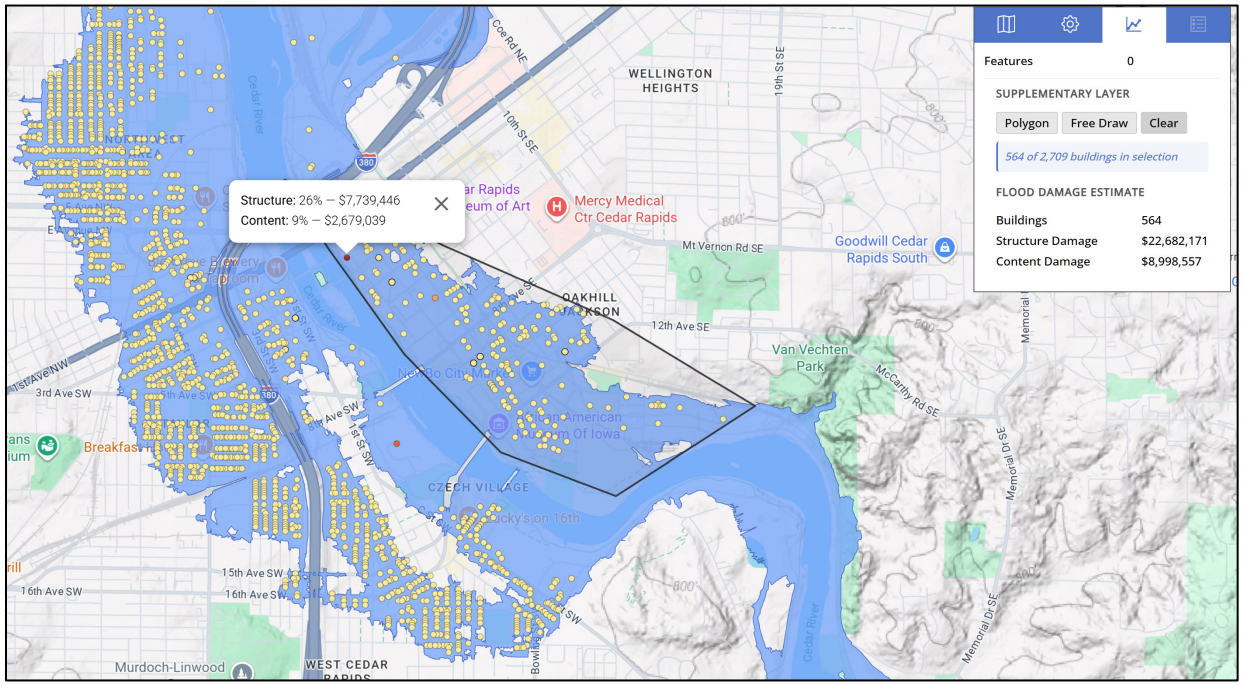


Figure 10. A flood damage layer is overlaid on a Cedar Rapids flood scenario layer, which has been added as a supplementary layer. This damage file is in the FIM Damage Format. Marker color reflects the combined structural and content damage of each property from yellow (low) to purple (severe), and the summary panel reports the aggregate damage and affected population for the scenario.

2.2.5. Layer Settings

The styling and behavior of every layer activated in FIMApp can be controlled based on user preferences. The user can also complete pixel-level inspection and get quantitative statistics for the layer based on pixel or regional values. For raster layers, the user can set options in the Layer Settings tab to control pixel color scales. The raster may be recolored using any of eight built-in palettes (Blue Scale, Grayscale, Rainbow, Heat, Viridis, Terrain, Reds, and Plasma), stretched across its value range and applied either as a few discrete color bands or as a smooth continuous gradient. Where the source GeoTIFF carries its own color legend in its GDAL_METADATA tag, the user may instead color the layer with that authoritative embedded theme. A hover option displays the underlying pixel value, with its unit where known, in a tooltip that tracks the cursor.

Correspondingly for vector layers, the color fill can be one of seven preset colors (each pairing a fill with a complementary stroke) at an adjustable fill opacity. For KML and KMZ files, which may carry their own per-feature styling, an option restores the colors defined in the file in place of the preset theme, and a hover option reveals a feature's attributes on mouse-over. Figure 11 shows a raster and vector sample for these features.

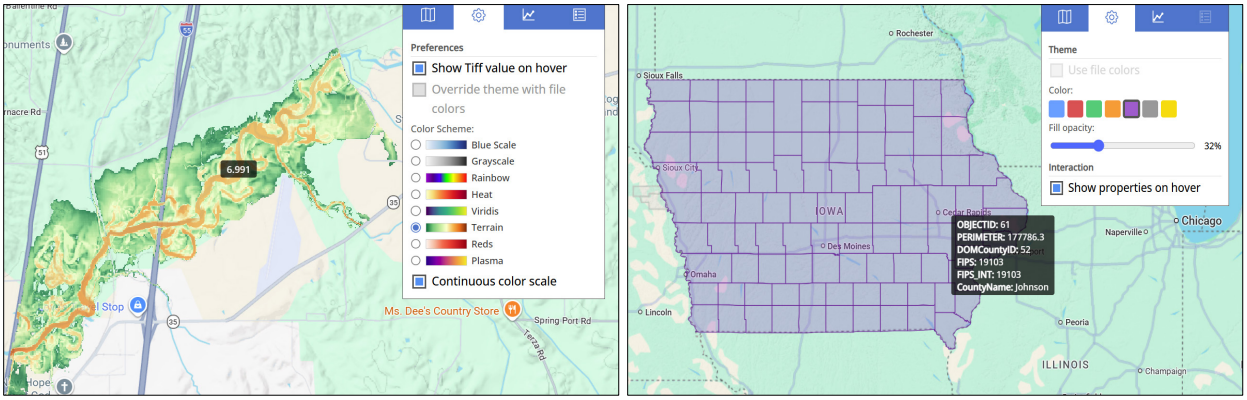


Figure 11. Layer styling controls. Raster layers (left) are recolored by palette and custom theme, with a pixel-value hover read-out; vector layers (right) are styled by custom color and opacity, with a feature-attribute hover read-out.

The Metrics tab summarizes the active layer quantitatively, computing its statistics only when the tab is first opened so that computational costs do not degrade layer loading performance. For rasters, it reports the minimum, maximum, mean, median, and standard deviation of the pixel values together with the count of valid pixels, annotated with the layer's unit where one is known; for vectors, it reports the feature count and geometry-type breakdown, and, where applicable, the total polygon area and line length computed on the ellipsoid. Velocity fields and damage layers report the type-specific quantities described in their respective sections.

For rasters and damage layers the tab also offers a region-of-interest tool: the user delimits an area by drawing a polygon or an enclosed freehand region, and the statistics are recomputed over only the pixels or properties inside it, allowing localized analyses rather than whole-layer statistics, as shown in Figure 12. This makes it straightforward to evaluate, for example, the mean inundation depth or the total estimated damage for a single neighborhood rather than the whole watershed region.

To support side-by-side interpretation of two datasets, FIMApp allows a second user file to be displayed simultaneously with the primary layer as a supplementary layer in User Files. Any previously uploaded file (other than the primary layer itself) may be selected and drawn over the current view and given its own parallel set of controls, mirroring those of the corresponding primary layer type but kept visually distinct so the two layers can be told apart. This makes it possible, for instance, to overlay a damage dataset on a flood-depth raster as shown in Figure 10. Each supplementary layer carries its own File Spec summary, styling controls, metrics, and legend, and can be added or removed on demand when viewing user files.

2.2.6. Comparison Sets

This functionality allows the user to upload two map layers and compare the overlap of the inundation areas. The two maps can either be vector or raster images and will be displayed on a single map-based interface. These files can either be obtained using the file uploader toolbox or by selecting two scenarios from any FIM Scenario file. If the uploaded files consist of one vector and one raster image, or two vector images, the interface lets users toggle between the two uploaded map layers to inspect overlaps and discrepancies between the two maps generated over the same geographic area. Figure 13 shows an example comparison of two flood maps at different stage levels for the Tallahatchie River.

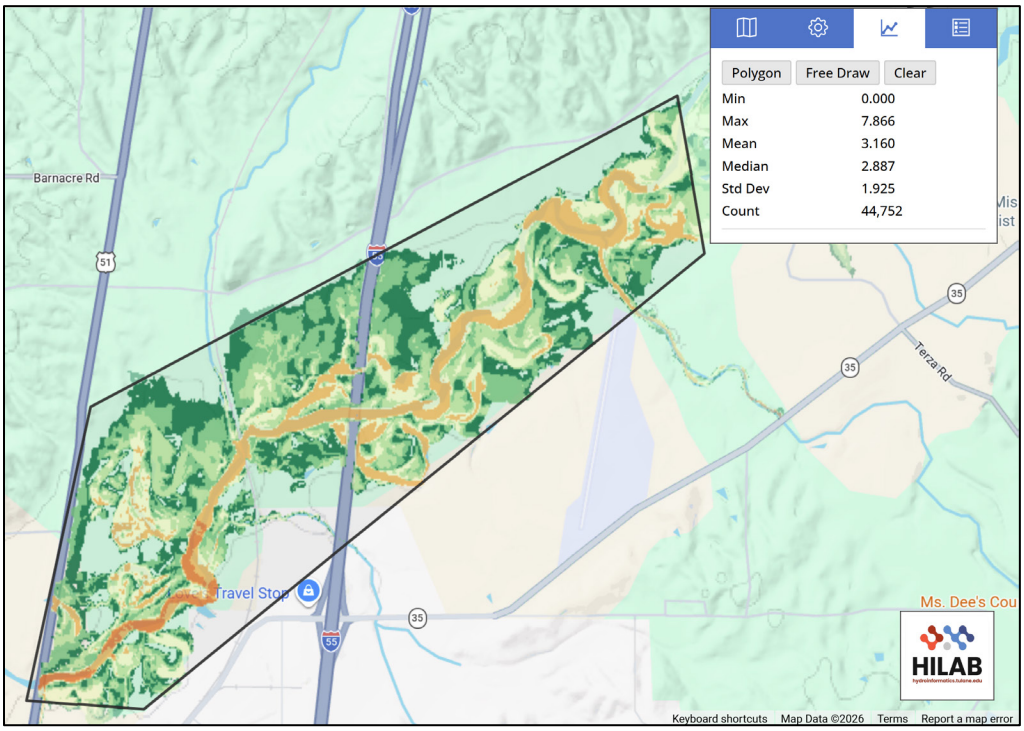


Figure 12. Region-of-interest metrics. A drawn polygon restricts the computed statistics to the selected area, reporting the pixel distribution for rasters, or the building count and aggregate losses for damage layers.

When the Comparison Set function is applied to two raster files, the application performs a pixel-wise comparison to identify intersecting inundation areas and regions unique to each map. The results display the polygon intersection area and overflow regions where the inundation extents do not overlap. For this comparison, both TIFF files must contain binary classification data with identical spatial properties. Each file should use pixel values of 0 (background) or 255 (foreground) in an 8-bit unsigned integer format. The datasets must also share the same WGS84 coordinate reference system, spatial resolution, bounding box, and pixel grid alignment to ensure direct pixel correspondence.

The two flood maps are overlaid and compared using a pixel-wise subtraction operation, which classifies each pixel into one of four categories: a) True Positive (TP): Both maps indicate inundation (foreground in both maps); b) False Positive (FP): The first map indicates inundation while the second indicates background (over-detection); c) False Negative (FN): The first map indicates background while the second indicates inundation (under-detection); and d) True Negative (TN): Both maps indicate background (no inundation in either map).

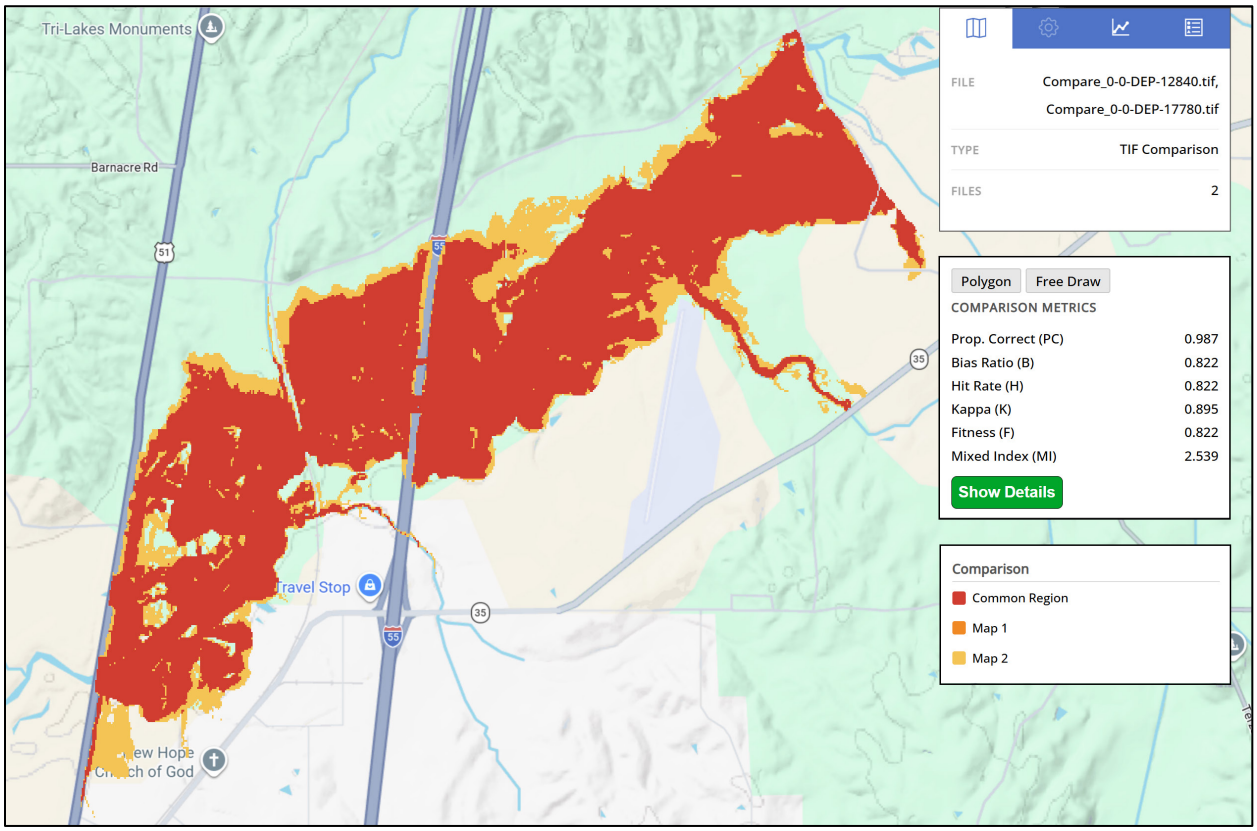


Figure 13. Comparison of two flood inundation scenarios for Tallahatchie River generated using two different inundation models and the results from the comparison metrics.

The metrics for evaluation, following Li et al. (2023), are as follows:

Proportion Correct (PC). Represents the overall accuracy of the comparison, measuring the fraction of pixels that are correctly classified in both positive and negative cases. It ranges from 0 to 1, where 1 indicates perfect agreement between the two maps (Eq 1).

$$PC = \frac{(TP + TN)}{(TP + FN + FP + TN)} \quad \text{Eq. 1}$$

Hit Rate (H). Also known as sensitivity or recall, measures the proportion of actual positive pixels (foreground in the reference map) that are correctly identified by the first map. It indicates how well the first map captures the features present in the reference map (Eq. 2).

$$H = \frac{TP}{(TP + FN)} \quad \text{Eq. 2}$$

Bias Ratio (B). Compares the total number of positive predictions in the first map to the total number of actual positives in the reference map. A value of 1 indicates no bias, values greater than 1 indicate over-prediction, and values less than 1 indicate under-prediction (Eq. 3).

$$B = \frac{(TP + FP)}{(TP + FN)} \quad \text{Eq. 3}$$

Fitness Statistic (F). Also known as the critical success index or Jaccard index, measures the overlap between the two maps while penalizing both false positives and false negatives. It provides a balanced measure of accuracy that is particularly useful when the classes are imbalanced (Eq. 4).

$$F = \frac{TP}{(TP + FP + FN)} \quad \text{Eq. 4}$$

Kappa Value (K). Measures the agreement between the two maps while accounting for chance agreement. It ranges from -1 to 1: 1 indicates perfect agreement, 0 indicates chance agreement, and negative values indicate agreement worse than chance (Eq. 5).

$$K = \frac{[N(TP + TN) - ((TP + FP) \times (TP + FN) + (FP + TN) \times (FN + TN))]}{[N^2 - ((TP + FP) \times (TP + FN) + (FP + TN) \times (FN + TN))]} \quad \text{Eq. 5}$$

Mixed Index (MI). A composite metric that combines Hit Rate, Kappa Value, and Fitness Statistics to provide an overall assessment of map comparison quality. Higher values indicate better agreement across multiple dimensions of accuracy (Eq. 6).

$$MI = H + K + F \quad \text{Eq. 6}$$

Once the files are loaded, FIMApp displays the common and exclusive regions of both flood maps along with summary comparison metrics.

2.2.7. Velocity Field Viewer

The Velocity Field Viewer animates two-dimensional flow fields, for example, depth-averaged flood-flow velocities produced by a hydrodynamic model, directly on the map. Whereas the other raster products encode a scalar quantity, a velocity field is a vector quantity and is supplied as a pair of single-band GeoTIFFs: an X (East–West) component and a Y (North–South) component,

sharing the same grid and extent. Both components are uploaded together to the interface, validated and/or reprojected, and stored in a single IndexedDB row.

When a velocity dataset is activated, the two component rasters are decoded and combined into a gridded vector field. The field is visualized as an animated particle flow: many short, moving streaks are seeded across the visible map area and advected along the local flow direction, producing an intuitive depiction of direction and relative speed. Each streak is colored by local speed magnitude using a four-grade light-to-dark blue scale, and the scale is dynamically normalized to the dataset's maximum speed so theEach streak is colored full color range is used regardless of the absolute velocities involved, as shown in Figure 14. The animation is drawn on a canvas overlay sized to the map; it pauses while the user pans or zooms and rebuilds for the new view once the map settles, ensuring the field always matches the current extent.

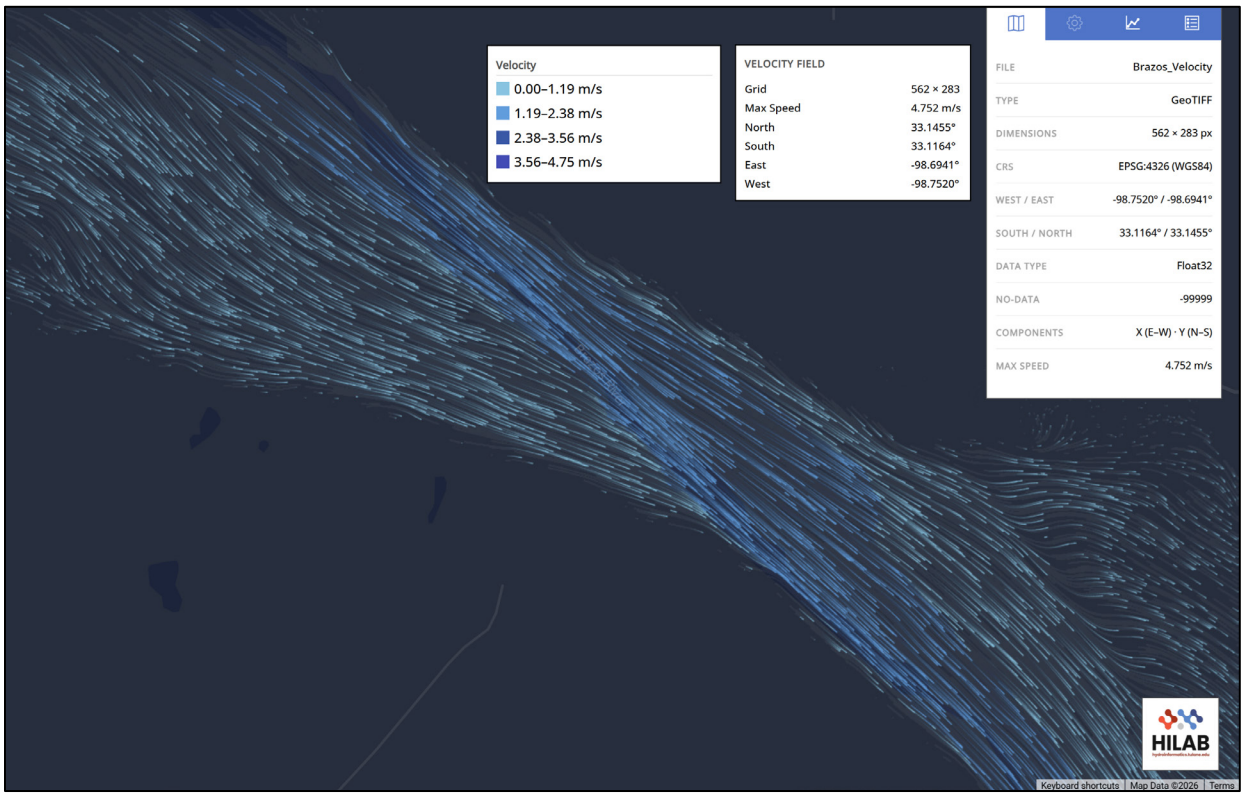


Figure 14. An animated velocity field for a scenario on the Brazos River. We have changed the map type to night to make moving particles easier to trace. Particle streak movement and color indicate velocity.

The velocity layer is managed through the same Layer Panel as the other layer products. Its File Spec tab reports the velocity field's grid dimensions, geographic bounds, and maximum speed; its Legend tab shows the speed color scale, with each blue grade labeled by its speed range in meters per second; and its Metrics tab summarizes the grid dimensions, maximum speed, and the north/south/east/west extent of the field. Embedded GeoTIFF metadata for the underlying components, where present, is also surfaced.

2.3. File Uploader Toolbox

The File Uploader Toolbox serves as the primary data ingestion layer of FIMApp, providing a centralized interface for importing geospatial datasets used across the application's map visualization layers. The toolbox supports multiple upload workflows, including retrieval from remote URLs, local filesystem uploads, and database queries, allowing users to integrate data from different sources. Uploaded datasets are stored in browser-based IndexedDB instances to enable efficient persistence and retrieval during application use. The toolbox implements five upload methods optimized for specific data types and workflows, as summarized in Table 2. The User File Viewer function enables visualization of uploaded inundation maps and other geospatial datasets within the Google Maps interface. Once data is ingested through the uploader, the viewer renders the datasets using the same loading mechanisms applied in the scenario-based visualization functions. This capability allows users to analyze additional geospatial data beyond predefined scenario files.

Table 2. List of available uploading and source types in the application.

Upload Type	Source	Purpose / Used By
FIM Database	URL	Loads a catalog of available files. Users select datasets to retrieve, which are then available in the User File Viewer.
FIM Scenario	URL or local file	Provides scenario datasets used in the Flood Extent (Scenario) and Flood Extent (Time Series) functions.
FIM Comparison	Local file or scenario selection	Uploads two geospatial datasets for use in the Comparison Set function.
Geospatial File	URL or local file	Imports general geospatial datasets including vector layers, raster images, depth maps, ensemble model outputs, and property-level damage datasets for visualization in the User File Viewer.
Velocity	Local file (paired X/Y GeoTIFFs)	Loads the two velocity components of a flow field for animated display in the Velocity Field Viewer.

FIMApp uses IndexedDB, a client-side NoSQL database available in modern web browsers, to store uploaded datasets locally within the user's browser. This approach allows structured and semi-structured geospatial data, including files, blobs, and JavaScript objects, to persist across browser sessions without requiring server-side storage. Using IndexedDB enables large geospatial datasets to be processed and visualized directly within the browser environment. By avoiding continuous server communication, the system reduces network latency and bandwidth usage while supporting responsive performance and limited offline functionality.

The application maintains a single versioned database (toolbox-store) whose schema organizes stored data into seven object stores, each corresponding to a specific application workflow: (i) filesMetadatageneral: geospatial datasets for the User File Viewer; (ii) filesCompareMetadata:

datasets used in the map comparison operation; (iii) filesFloodExtentMetadata: FIM Scenario files used in flood extent and time-series visualization; (iv) filesDamageMetadata: property-level damage datasets used for damage analysis; (v) filesDepthMetadata: flood-depth grids; (vi) filesEnsembleMetadata: ensemble model outputs; and (vii) filesVelocityMetadata: velocity-field components.

The application provides standard database operations for storing, retrieving, listing, and deleting files within these object stores. Database initialization includes version control and automatic object store creation to ensure compatibility across application updates. This client-side storage architecture allows FIMApp to manage geospatial datasets entirely within the browser, providing persistent storage and efficient access during visualization and analysis workflows.

3. Results and Discussion

3.1. Case Study 1: Stage-wise Inundation Mapping for Chickasawhay River, MS

This case study demonstrates stage-wise flood extent analysis for the Chickasawhay River in Mississippi, showing how inundation patterns evolve across different flood stages. The Chickasawhay River, a major tributary of the Pascagoula River basin, provides a representative floodplain for exploring spatial flood dynamics using the HAND methodology. For this analysis, a FIM Scenario file was created and loaded into the Flood Extent (Scenario) viewer within FIMApp. The scenario file includes flood stages ranging from 20 to over 40 feet, representing historical and potential major flooding events. Using the FIMApp interface, users can navigate between stages, visualize inundation patterns dynamically, and compare flood extent across stages.

This stage-wise mapping approach supports decision-making by allowing planners and emergency managers to identify thresholds at which critical infrastructure, communities, and ecological zones are affected as river stage rises. Further granular analyses are possible with pixel-wise data at point locations. By integrating time-series and damage visualization functions, stakeholders can also assess potential property impacts and explore mitigation strategies, including flood warning systems and cost-benefit analyses for proposed interventions (see Figure 15).

3.2. Case Study 2: Comparison of Flood Models for Batesville, MS: HAND vs. SRH-2D Modeling for a 50-year Flood Event

This case study evaluates spatial agreement between two flood modeling approaches for the Batesville area: the HAND model and the Sedimentation and River Hydraulics Two-Dimensional (SRH-2D) model (US Bureau of Reclamation, 2016). Both models produce GeoTIFF raster outputs, which were uploaded to FIMApp using the File Uploader Toolbox and analyzed with the Comparison Set function. The resulting comparison map (Figure 16) highlights areas of agreement and disagreement. Regions predicted as flooded by both models (True Positives, shown in red) indicate strong concordance, while limited orange (HAND-only) and yellow (SRH-2D-only) areas reveal minor spatial differences. Discrepancies occur in downstream or geometrically complex areas, where HAND either overpredicts or SRH-2D's detailed hydraulics capture nuanced flooding not detected by HAND.

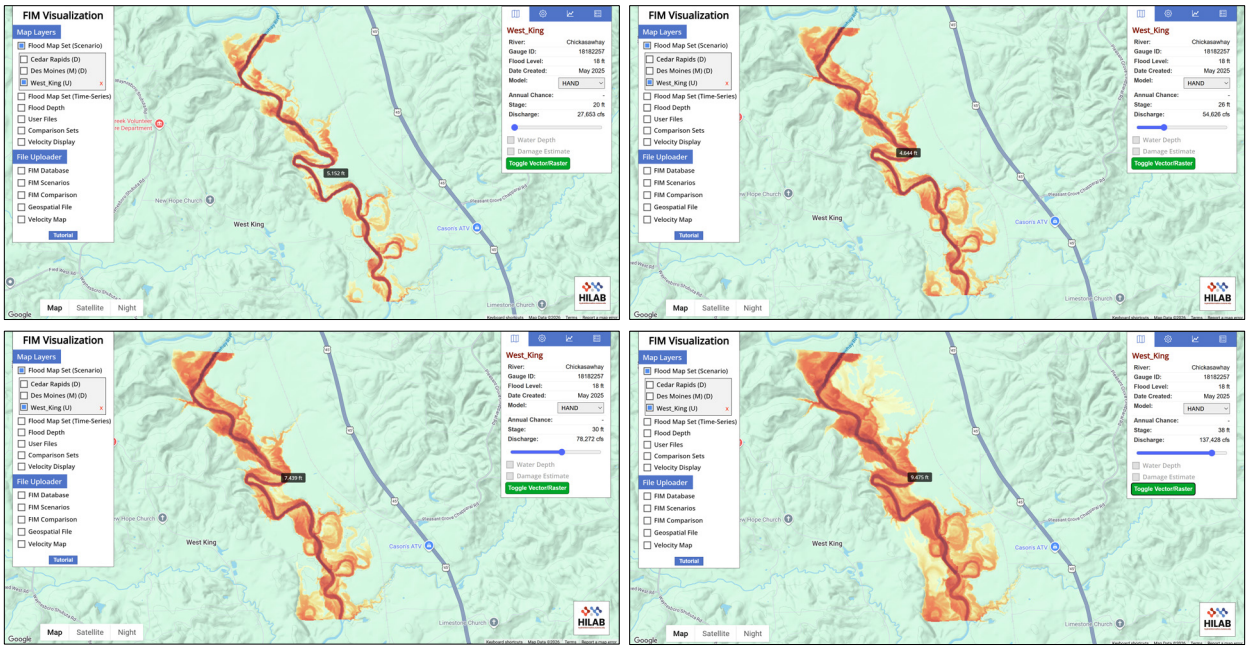


Figure 15. Flooding scenarios for the Chickasawhay River near West King, Mississippi, shown at four increasing stage levels (20 ft, 26 ft, 30 ft, and 38 ft) from top-left to bottom-right respectively. The maps illustrate critical thresholds with inundation spreading into surrounding areas.

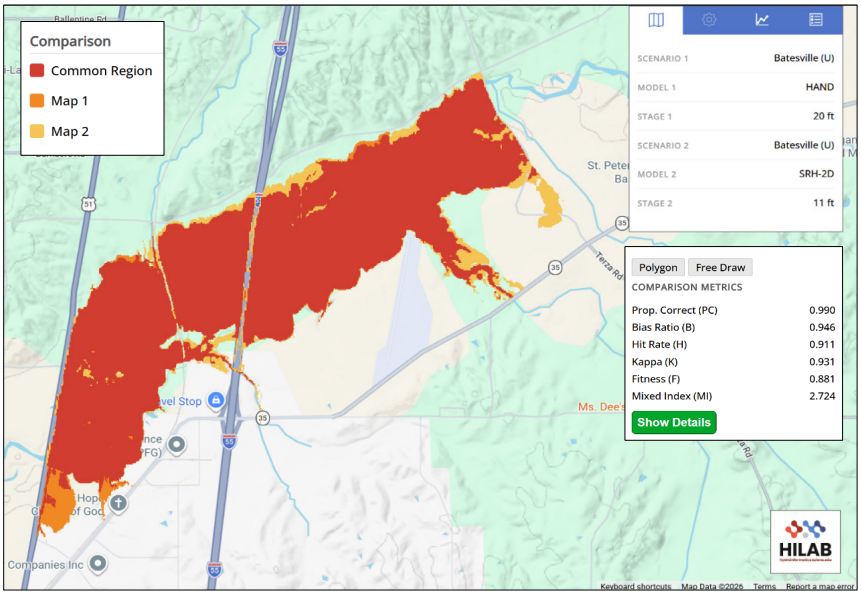


Figure 16. Pixelwise comparison for 50-year flood scenario for Batesville using HAND and SRH-2D models.

Quantitative comparison metrics confirm this agreement. A Proportion Correct of 0.99 indicates near-perfect spatial overlap, a Bias Ratio of 0.95 shows minimal systematic difference, and a Hit Rate of 0.91 confirms that HAND captures most flood-prone areas identified by SRH-2D. The Kappa value of 0.93 indicates substantial agreement beyond chance, the Fitness Statistic

of 0.88 reflects excellent overlap, and the Mixed Index of 2.72 represents high composite accuracy among the datasets. These results suggest that the terrain-based HAND approach can reliably reproduce flood extents comparable to more computationally intensive SRH-2D modeling. Despite differences in stage levels (11-foot vs 20-foot), both models produce similar spatial patterns, reflecting the influence of local floodplain geometry on inundation dynamics.

3.3. Case Study 3: Distributing the BYU FIM Database through HydroShare

The BYU FIM Database provides a real-world example of structuring, storing, and accessing flood datasets using HydroShare. This case study demonstrates how the FIM Database format (Section 2.1) supports reproducible, scalable flood mapping workflows and facilitates data sharing across projects and users. The database hosted on HydroShare includes a JSON file, FIMDatabase.json, which catalogs multiple flood inundation layers generated using models from USACE (ERDC), Mississippi DOT, AutoRoute, and the satellite-based FIER framework (Markert et al., 2026; Prince et al., 2025), as cataloged by Oldham et al. (2024) and described in detail by Wagle et al. (2026). Each entry corresponds to a flood scenario file with associated metadata, allowing systematic organization of datasets.

The database was developed at Brigham Young University under the Cooperative Institute for Research to Operations in Hydrology (CIROH) to complement the National Water Center's operational NWM HAND product with flood maps produced by other agencies and methods (Oldham, 2025; Wagle et al., 2026). Its contents fall into three groups: maps harvested from public agency inventories (FEMA National Flood Hazard Layer polygons, InFRM and USGS stage-based inundation libraries, and remotely sensed benchmark maps from the Surface Dynamics Modeling Lab (Devi et al., 2025)); outputs collected from agency-built hydraulic models (USACE HEC-RAS 2D and state transportation department SRH-2D models); and maps generated by the BYU group to fill gaps, including AutoRoute (Follum, 2013) and FIER extents and a baseline NWM HAND map for every site, produced with the FIMserv tool (Baruah et al., 2025) for the 2- through 100-year return period flows. Because these products arrive in different projections, data types, resolutions, and file structures, each passes through a standardization workflow before cataloging. Rasters are converted to Float32 GeoTIFF, reprojected to WGS84 (EPSG:4326), assigned a common NoData value, aligned to a shared pixel grid, and losslessly compressed, which reduced average file sizes by more than 60% for every model type; vector extents are dissolved to a single polygon and boundary-smoothed. Files follow a "{Model}_{ReachID}_{discharge}_{unit}_{type}" naming convention so that metadata can be generated automatically.

Alongside the map files, the database records the metadata needed to interpret and retrieve them. A relational schema of eight linked tables stores, for each FIM source, the generating model and version, the responsible entity and contact, the rating curve relating discharge, depth, and return period to each file, the HUC8 watershed, and the list of NWM reach identifiers that fall within the map domain (Wagle et al., 2026). The NWM reach link allows a forecast discharge to match the nearest stored flood map, using the same nearest-stage matching that FIMApp applies

to the time-series entries of the FIM Scenario format (Section 2.1). Each published HydroShare resource also carries JSON index files that expose the model's name, return period, discharge, and file URLs to the web viewer; the FIMDatabase.json catalog read by FIMApp is one of these. The pixel-aligned WGS84 grids produced by the standardization step also satisfy the grid-correspondence requirement of the Comparison Set function (Section 2.2), so maps from different sources in the database can be compared directly. A companion demonstration using this database compares HAND and SRH-2D extents for the Tallahatchie River, Mississippi, through the scenario viewer and comparison tool (Wagle et al., 2026), the same river shown in Figure 13.

Loading the database into FIMApp enables users to browse and retrieve individual files, which are stored in the browser's IndexedDB for access via the User File Viewer (Figure 17). By appending the referenced file name to the HydroShare resource URL, any inundation layer can be directly retrieved by FIMApp or other client-side tools. Leveraging HydroShare (Tarboton et al., 2024) ensures persistent data hosting, version control, and standardized metadata, simplifying discovery, retrieval, and integration of flood scenario data. This case study illustrates how the FIM Database format and FIMApp together enable efficient, reproducible workflows for flood mapping and scenario analysis.

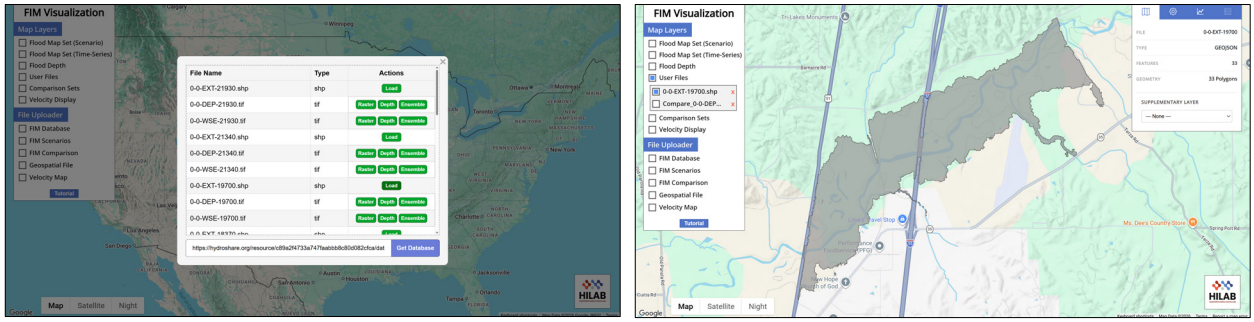


Figure 17. Loading, storing, and viewing a file from the BYU FIM Database using the FIM Database function.

3.4. Limitations

While FIMApp provides a flexible, lightweight, and accessible framework for flood inundation visualization, its client-side, browser-based design introduces several limitations. First, computation and rendering performance depend heavily on the user's hardware and browser capabilities. Complex raster datasets, large GeoTIFFs, and multi-layer comparisons may lead to slow rendering, increased memory usage, or reduced responsiveness on lower-end devices. Unlike server-side processing pipelines, the browser environment restricts parallel computation and limits opportunities for optimized geoprocessing, particularly for operations such as pixel-wise raster comparison or dynamic depth calculations.

Second, FIMApp relies on browser-managed storage through IndexedDB, which imposes practical limits on the volume and size of datasets that can be persistently stored. Storage quotas vary across browsers and devices, and in some cases, the browser may automatically purge stored data to reclaim space. These constraints limit the long-term caching of flood scenario libraries or

high-resolution model outputs. Third, dataset accessibility depends on remote file availability, user-provided URLs, and cross-origin permissions. When external servers enforce strict CORS policies, restrict HTTPS access, or change resource paths, dataset retrieval may fail. This dependency can hinder reproducibility and requires users to ensure stable hosting of their geospatial files. Additionally, large remote datasets may introduce latency during fetching and decoding, particularly over limited network connections. Server-side services that expose subsets of large-extent spatial datasets hosted on HydroShare offer one way to reduce this burden (Choi et al., 2025).

Finally, although FIMApp introduces portable JSON-based formats to describe flood scenarios, metadata, and property-level damage, broader community adoption of such standards remains limited. Such uptake depends as much on trust and sustained engagement with users as on technical design (Sowby et al., 2025). Existing flood mapping datasets often use heterogeneous formats that omit critical metadata (e.g., datum references, scenario semantics, boundary conditions, or model configurations), reducing interoperability across tools. While the proposed FIM Database, Scenario, and Damage specifications improve clarity and portability, consistent standardization across institutions, modeling frameworks, and data repositories is still an ongoing need. This gap highlights both the importance and the challenge of establishing community-oriented schemas to represent inundation scenarios transparently and reproducibly.

4. Conclusion and Future Work

This study introduced the Flood Inundation Mapping Application (FIMApp), a robust, client-side web application for uploading, visualizing, analyzing, and comparing flood maps using scalable, reproducible data formats. The platform supports scenario-based flood-extent visualization, time-series analysis, flood-depth mapping, flood-damage estimation, and comparative evaluation of different inundation modeling techniques. It relies on standardized, JSON-based data structures, including FIM Database, FIM Scenario, and FIM Damage, to promote interoperability with existing hydrologic databases and modeling frameworks. Coupled with IndexedDB for client-side storage, the system efficiently manages large geospatial datasets, providing responsive performance and offline functionality.

Case studies demonstrate the platform's utility. Stage-wise inundation mapping for the Chickasawhay River highlighted critical thresholds for infrastructure and community vulnerability, while comparative analysis of HAND and SRH-2D models in Batesville quantified spatial agreement and model accuracy using statistical metrics. Integration with the BYU FIM Database illustrates the scalability of standardized formats and facilitates collaboration through HydroShare-hosted datasets.

Future development will expand visualization options, including multi-band rasters and three-dimensional surface elevation, to support additional file formats and enhance comparison capabilities beyond single-band raster images. Incorporating real-time forecasting, machine-learning-based predictive flood-damage modeling, and additional online flood datasets could further extend analytical capabilities. Adapting the system as a JavaScript library would allow

integration of its visualization tools into other geospatial applications. Optimizing the application's responsiveness for mobile or tablet use would help increase usage among mobile users. Continuous community-driven feedback will guide iterative improvements, ensuring the platform remains a valuable resource for researchers, planners, and emergency managers engaged in flood risk assessment and mitigation.

Declaration of Generative AI and AI-Assisted Technologies

During the preparation of this work, the authors used ChatGPT and Claude to develop the software herein described and improve readability throughout the manuscript. The authors also used Grammarly to improve the writing. After using these tools, the author(s) reviewed and edited the content as needed and took full responsibility for the content of the publication.

CRediT Author Statement

Moiyyad Sufi: Conceptualization, Data Curation, Formal Analysis, Investigation, Methodology, Writing – Original Draft. **Carlos Erazo Ramirez:** Conceptualization, Writing – review & editing. **Felipe Quintero:** Writing – review & editing. **Bong-Chul Seo:** Writing – review & editing. **Pitamber Wagle:** Writing – review & editing. **Dan Ames:** Conceptualization, Funding acquisition, Writing – review & editing. **Jim Nelson:** Conceptualization, Funding acquisition, Writing – review & editing. **Ibrahim Demir:** Conceptualization, Formal analysis, Funding acquisition, Methodology, Supervision, Writing – review & editing.

5. Data and Software Availability

Name	Flood Inundation Mapping Application (FIMApp)
Developers	Moiyyad Sufi
Contact Information	https://hydroinformatics.tulane.edu
Software and Programming languages	Web Browser, JavaScript, HTML, CSS
Platform Access	https://hydroinformatics.tulane.edu/lab/fims/
Data	Example datasets are retrieved within the platform. The BYU FIM Database is openly available on HydroShare (Oldham et al., 2024).

6. References

Ames, D. P. (2026). Mapping water: A brief history of GIS in hydrology and a path toward AI-native modeling. Water, 18(7), 796. https://doi.org/10.3390/w18070796

Ames, D. P., Cohen, S., Clemins, P. J., Demir, I., Halgren, J., Horsburgh, J. S., Nelson, E. J., Patel, A., Read, J. S., Swain, N., & Tarboton, D. G. (2026). Bridging the research-to-operations gaps in NOAA water prediction through advances in hydroinformatics. Journal of the American Water Resources Association. In press.

Aristizabal, F., Salas, F., Petrochenkov, G., Grout, T., Avant, B., Bates, B., Spies, R., Chadwick, N., Wills, Z., & Judge, J. (2023). Extending Height Above Nearest Drainage to model multiple fluvial sources in flood inundation mapping applications for the U.S. National Water Model. Water Resources Research, 59(5). https://doi.org/10.1029/2022WR032039

Ashby, K. R., Hales, R. C., Nelson, E. J., Ames, D. P., & Williams, G. P. (2021). Hydroviewer: A web application to localize global hydrologic forecasts. Open Water Journal, 7(1), Article 9.

Baruah, A., Dhital, S., Cohen, S., et al. (2025). FIMserv v.1.0: A tool for streamlining flood inundation mapping (FIM) using the United States operational hydrological forecasting framework. Environmental Modelling & Software, 192, 106581. https://doi.org/10.1016/j.envsoft.2025.106581

Bates, P. D., Horritt, M. S., & Fewtrell, T. J. (2010). A simple inertial formulation of the shallow water equations for efficient two-dimensional flood inundation modelling. Journal of Hydrology, 387(1–2), 33–45. https://doi.org/10.1016/j.jhydrol.2010.03.027

Choi, Y., Maghami, I., Goodall, J. L., Band, L., Nassar, A., Lin, L., Saby, L., Li, Z., Wang, S., Calloway, C., Yi, H., Seul, M., Ames, D. P., & Tarboton, D. G. (2025). Toward reproducible and interoperable environmental modeling: Integration of HydroShare with server-side methods for exposing large-extent spatial datasets to models. Environmental Modelling & Software, 183, 106239. https://doi.org/10.1016/j.envsoft.2024.106239

Cikmaz, B. A., Yildirim, E., & Demir, I. (2025). Flood susceptibility mapping using fuzzy analytical hierarchy process for Cedar Rapids, Iowa. *International Journal of River Basin Management*, *23*(1), 1-13.

Cosgrove, B., D. Gochis, T. Flowers, A. Dugger, F. Ogden, T. Graziano, E. Clark, R. Cabell, N. Casiday, Z. Cui, K. Eicher, G. Fall, X. Feng, K. Fitzgerald, N. Frazier, C. George, R. Gibbs, L. Hernandez, D. Johnson, R. Jones, L. Karsten, H. Kefelegn, D. Kitzmiller, H. Lee, Y. Liu, H. Mashriqui, D. Mattern, A. McCluskey, J. L. McCreight, R. McDaniel, A. Midekisa, A. Newman, L. Pan, C. Pham, A. RafieeiNasab, R. Rasmussen, L. Read, M. Rezaeianzadeh, F. Salas, D. Sang, K. Sampson, T. Schneider, Q. Shi, G. Sood, A. Wood, W. Wu, D. Yates, W. Yu, and Y. Zhang. 2024. "NOAA's National Water Model: Advancing Operational Hydrology through Continental-Scale Modeling." *Journal of the American Water Resources Association (JAWRA)* 60 (2): 247-272. https://doi.org/10.1111/1752-1688.13184

Demir, I., Yildirim, E., Sermet, Y., & Sit, M. A. (2018). FLOODSS: Iowa Flood Information System as a generalized flood cyberinfrastructure. *International Journal of River Basin Management,* 16(3), 393–400. https://doi.org/10.1080/15715124.2017.1411927

Devi, D., Dhital, S., Munasinghe, D., et al. (2025). A framework for the evaluation of flood inundation predictions over extensive benchmark databases. ESS Open Archive preprint. https://doi.org/10.22541/essoar.175105672.23211828

Duran, E., Alabbad, Y., Mount, J., Yildirim, E., & Demir, I. (2025). Comprehensive analysis of riverine flood impact on bridge and transportation network: Iowa case study. *International Journal of River Basin Management*, 1-14.

ECMA. (2017). The JSON data interchange syntax (ECMA-404, 2nd ed.). https://ecma-international.org/wp-content/uploads/ECMA-404_2nd_edition_december_2017.pdf

Erazo Ramirez, C., Sermet, Y., Molkenthin, F., & Demir, I. (2022). HydroLang: An open-source web-based programming framework for hydrological sciences. *Environmental Modelling & Software,* 157, 105525. https://doi.org/10.1016/j.envsoft.2022.105525

Erazo Ramirez, C., Sermet, Y., & Demir, I. (2023). HydroLang markup language: Community-driven web components for hydrological analyses. *Journal of Hydroinformatics*, 25(4), 1171-1187. https://doi.org/10.2166/hydro.2023.149

Erazo Ramirez, C., & Demir, I. (2025). AI-assisted voice enabled computing framework for hydrological analysis. *Environmental Modelling & Software*, 106833.

Ewing, G., Mantilla, R., Krajewski, W., & Demir, I. (2022). Interactive hydrological modelling and simulation on client-side web systems: An educational case study. *Journal of Hydroinformatics*, 24(6), 1194-1206.

Follum, M. L. (2013). AutoRoute rapid flood inundation model (ERDC/CHL CHETN-IV-88). U.S. Army Engineer Research and Development Center. https://apps.dtic.mil/sti/html/tr/ADA583052/

GIS Analysis & Support. (2025). Department of Natural Resources. Retrieved July 30, 2025, from https://www.iowadnr.gov/programs-services/gis-analysis-support

Gilles, D., Young, N., Schroeder, H., Piotrowski, J., & Chang, Y.-J. (2012). Inundation Mapping Initiatives of the Iowa Flood Center: Statewide Coverage and Detailed Urban Flooding Analysis. *Water*, *4*(1), 85-106. https://doi.org/10.3390/w4010085

Hales, R. C., Nelson, E. J., Souffront, M., Gutierrez, A. L., Prudhomme, C., Kopp, S., Ames, D. P., Williams, G. P., & Jones, N. L. (2022). Advancing global hydrologic modeling with the GEOGloWS ECMWF streamflow service. Journal of Flood Risk Management, e12859. https://doi.org/10.1111/jfr3.12859

Horsburgh, J. S., Morsy, M. M., Castronova, A. M., Goodall, J. L., Gan, T., Yi, H., Stealey, M. J., & Tarboton, D. G. (2015). HydroShare: Sharing diverse environmental data types and models as social objects with application to the hydrology domain. JAWRA Journal of the American Water Resources Association, 52(4), 873-889. https://doi.org/10.1111/1752-1688.12363

Johnson, J. M., Munasinghe, D., Eyelade, D., & Cohen, S. (2019). An integrated evaluation of the NWM–HAND flood mapping methodology. Natural Hazards and Earth System Sciences, 19(11), 2405–2420. https://doi.org/10.5194/nhess-19-2405-2019

Kumar, V., Sharma, K. V., Caloiero, T., Mehta, D. J., & Singh, K. (2023). Comprehensive overview of flood modeling approaches: A review of recent advances. Hydrology, 10(7), 141. https://doi.org/10.3390/hydrology10070141

Li, Z., Mount, J., & Demir, I. (2022). Accounting for uncertainty in real time flood inundation mapping using HAND: Iowa case study. Natural Hazards, 112(1), 977–1004. https://doi.org/10.1007/s11069-022-05215-z

Li, Z., Duque, F. Q., Grout, T., Bates, B., & Demir, I. (2023). Comparative analysis of performance and mechanisms of flood inundation map generation using Height Above Nearest Drainage. *Environmental Modelling & Software*, *159*, 105565.

Li, Z., Sermet, Y., & Demir, I. (2025). EarthObsNet: A comprehensive Benchmark dataset for data-driven earth observation image synthesis. *Environmental Modelling & Software*, *185*, 106292.

Maghami, I., Ames, D. P., Aghababaei, A., Chapagain, A. R., Anderson, J. M., & Garcia, J. J. (2026). How well do U.S. National Water Model short-range forecasts predict flood event timing and magnitude? Journal of Hydrology: Regional Studies, 64, 103108. https://doi.org/10.1016/j.ejrh.2026.103108

Mahjarin, T., Krewson, C., Swain, N., Shi, J., & Ames, D. P. (2026). Tethys Dash: An open-source low-code platform for hydrologic visualization and integrated decision support. Journal of Hydroinformatics, jh2026164. https://doi.org/10.2166/hydro.2026.164

Map service. (2025). Esri Developer. Retrieved July 30, 2025, from https://developers.arcgis.com/rest/services-reference/enterprise/map-service

Markert, K. N., Lee, H., Williams, G. P., Nelson, E. J., Ames, D. P., Griffin, R. E., & Meyer, F. J. (2026). Evaluating the feasibility of scaling the FIER framework for large-scale flood inundation prediction. Hydrology and Earth System Sciences, 30, 459–484. https://doi.org/10.5194/hess-30-459-2026

Neal, J. C., Dunne, T., Sampson, C., Smith, A., & Bates, P. (2018). Optimisation of the two-dimensional hydraulic model LISFLOOD-FP for CPU architecture. Environmental Modelling & Software, 107, 148–157. https://doi.org/10.1016/j.envsoft.2018.05.011

NOAA Office of Water Prediction. (2025). Inundation Mapping. GitHub. https://github.com/NOAA-OWP/inundation-mapping

Nobre, A. D., Cuartas, L. A., Hodnett, M., Rennó, C. D., Rodrigues, G., Silveira, A., Waterloo, M., & Saleska, S. (2011). Height Above the Nearest Drainage—A hydrologically relevant new terrain model. Journal of Hydrology, 404(1–2), 13–29. https://doi.org/10.1016/j.jhydrol.2011.03.051

Oldham, S., Nelson, J., & Prince, L. (2024). BYU FIM Database Optimized for Web Viewers. HydroShare. http://www.hydroshare.org/resource/c89a2f4733a747faabbb8c80d082cfca

Oldham, S. J. (2025). A multi-model and multi-agency approach to expand the flood inundation mapping capacity of the US National Water Center [Master's thesis, Brigham Young University]. BYU ScholarsArchive. https://scholarsarchive.byu.edu/etd/10683

OpenTELEMAC Consortium / EDF. (2000). TELEMAC 2D: Validation document (v5.0). https://www.opentelemac.org/downloads/MANUALS/TELEMAC-2D/vali50_gb.pdf

OpenTELEMAC Consortium / EDF. (2012). TELEMAC 2D: Reference manual (v6p2). https://www.opentelemac.com/index.php/component/jdownloads/summary/13-telemac-2d/178-telemac-2d-reference-manual-en-v6p2

Prince, L., Hales, R. C., Markert, K. N., Nelson, E. J., Williams, G. P., Ames, D. P., Lee, H., & Rostami, A. (2025). Assessing coincidence of satellite acquisitions and flood events to predict for flood map synthesis. Remote Sensing, 17(9), 1648. https://doi.org/10.3390/rs17091648

Rojas-Lesmes, D., Sanchez-Lozano, J., Nelson, E. J., Chancay-Sanchez, J., Rodriguez-Chaves, J., Larco-Erazo, K., Romero, E. G., Trujillo-Vela, M., Hales, R. C., Ames, D. P., & Gutierrez, A. L. (2025). National Water Level Forecast (NWLF): An open-source customizable web application for the GEOGLOWS ECMWF global hydrological model. Information Geography, 1, 100008. https://doi.org/10.1016/j.infgeo.2025.100008

Scawthorn, C., Flores, P., Blais, N., Seligson, H., Tate, E., Chang, S., Mifflin, E., Thomas, W., Murphy, J., Jones, C., & Lawrence, M. (2006). HAZUS-MH flood loss estimation methodology. II. Damage and loss assessment. *Natural Hazards Review*, *7*(2), 72-81. https://doi.org/10.1061/(asce)1527-6988(2006)7:2(72)

Seneviratne, S. I., Zhang, X., Adnan, M., Badi, W., Dereczynski, C., Luca, A. D., Ghosh, S., Iskandar, I., Kossin, J., Lewis, S., Otto, F., Pinto, I., Satoh, M., Vicente-Serrano, S. M., Wehner, M., Zhou, B., & Allan, R. (2021). Weather and climate extreme events in a changing climate. Climate Change 2021: The Physical Science Basis: Working Group I contribution to the Sixth Assessment Report of the Intergovernmental Panel on Climate Change, 1513-1766. https://doi.org/10.1017/9781009157896.013

Shustikova, I., Domeneghetti, A., Neal, J. C., Bates, P., & Castellarin, A. (2019). Comparing 2D capabilities of HEC-RAS and LISFLOOD-FP on complex topography. *Hydrological Sciences Journal*, *64*(14), 1769-1782.

Sowby, R., South, A., Hopkins, E., Jones, N. L., & Ames, D. P. (2025). More than modeling: Building trust for positive change in water resources management. Environmental Modelling & Software, 189, 106465. https://doi.org/10.1016/j.envsoft.2025.106465

Sufi, M., Erazo Ramirez, C., & Demir, I. (2025). Hydrolang FRAM: Web-based framework for comprehensive flood risk and mitigation assessment and communication. *International Journal of Disaster Risk Reduction*, 105735.

Sugiyama, K., Erazo Ramirez, C., & Demir, I. (2025). Community-Oriented Data Integration and Communication Framework for Streamflow Forecast Models and Flood Inundation Map Products. *EarthArXiv preprint.* https://doi.org/10.31223/X5JJ31

Swain, N. R., Christensen, S. D., Snow, A. D., Dolder, H., Espinoza-Dávalos, G., Goharian, E., Jones, N. L., Nelson, E. J., Ames, D. P., & Burian, S. J. (2016). A new open source platform for lowering the barrier for environmental web app development. Environmental Modelling & Software, 85, 11–26. https://doi.org/10.1016/j.envsoft.2016.08.003

Tarboton, D. G., Ames, D. P., Horsburgh, J. S., Goodall, J. L., Couch, A., Hooper, R., Bales, J., Wang, S., Castronova, A., Seul, M., Idaszak, R., Li, Z., Dash, P., Black, S., Ramirez, M., Yi, H., Calloway, C., & Cogswell, C. (2024). HydroShare retrospective: Science and technology advances of a comprehensive data and model publication environment for the water science domain. Environmental Modelling & Software, 172, 105902. https://doi.org/10.1016/j.envsoft.2023.105902

Thalakkottukara, N. T., Thomas, J., Watkins, M. K., et al. (2024). Suitability of the Height Above Nearest Drainage (HAND) model for flood inundation mapping in data-scarce regions: A comparative analysis with hydrodynamic models. Earth Science Informatics, 17, 1907–1921. https://doi.org/10.1007/s12145-023-01218-x

Trenberth, K. E., Fasullo, J. T., & Shepherd, T. G. (2015). Attribution of climate extreme events. Nature Climate Change, 5(8), 725-730. https://doi.org/10.1038/nclimate2657

US Bureau of Reclamation (2016). Modeling in-stream structures and internal features with SRH-2D (SRH-2016-09). https://www.usbr.gov/tsc/techreferences/mands/mands-pdfs/ModelingIn-StreamStructuresInternalFeaturesWith%20SRH-2D_02-2016_508.pdf

USACE HEC. (2016). HEC-RAS River Analysis System: Hydraulic Reference Manual (v5.0, CPD-69).http://caee.webhost.utexas.edu/prof/maidment/ce365kspr16/HEC/HEC-RAS5.0ReferenceManual.pdf

Wagle, P., Oldham, S. J., Nelson, E. J., Hales, R. C., Hotchkiss, R. H., Ames, D. P., Demir, I., Sufi, M., Prince, L., Larco, K., & Miskin, T. (2026). Integrating modeled flood maps from the National Water Model and diverse sources for enhanced forecasting and preparedness. Journal of the American Water Resources Association, 62(2), e70107. https://doi.org/10.1111/1752-1688.70107